Genome sequencing and neurotoxin diversity of a wandering spider *Pardosa pseudoannulata* (pond wolf spider)

Na Yu[1,&], Jingjing Li[1,&], Meng Liu[2,&], Lixin Huang[1], Haibo Bao[1], Zhiming Yang[1], Yixi Zhang[1], Haoli Gao[1], Zhaoying Wang[1], Yuanxue Yang[1], Thomas Van Leeuwen[3], Neil S. Millar[4], Zewen Liu[1,*]

1, Key laboratory of Integrated Management of Crop Diseases and Pests (Ministry of Education), College of Plant Protection, Nanjing Agricultural University, Weigang 1, Nanjing 210095, China

2, Novogene Bioinformatics Institute, Beijing 100083, China

3, Faculty of Bioscience Engineering, Ghent University, Coupure links 653, Ghent B9000, Belgium

4, Department of Neuroscience, Physiology & Pharmacology, University College London, Gower Street, London WC1E 6BT, United Kingdom

*, Correspondence should be addressed to Zewen Liu (Key laboratory of Integrated Management of Crop Diseases and Pests (Ministry of Education), College of Plant Protection, Nanjing Agricultural University, Weigang 1, Nanjing 210095, P.R. China, Tel: -86 25 84399051; E-mail: liuzewen@njau.edu.cn.

&, these authors contributed equally and should be regarded as co-first authors.

Abstract

Spiders constitute an extensive and diverse branch of the phylum Arthropoda. Whereas the genomes of four web-weaver spider species and a single cave-living spider have been determined, similar studies have not been reported previously for a wandering spider. The pond wolf spider, *Pardosa pseudoannulata*, is a wandering hunter that immobilizes prey using venom rather than a web. It is also an important predator against a range of agriculturally important insect pests. The increasing interest in its wandering lifestyle and in the potential of spider venom as a tool for pest control have prompted a detailed study on this wandering spider species. We have generated a high-quality genome sequence of *P. pseudoannulata* and analysed genes associated with the production of silk and venom toxins. Sequencing reveals that *P. pseudoannulata* has a large genome of 4.26 Gb. The presence of only 16 spidroin genes and four types of silk glands is consistent with the moderate use of silk and the lack of a prey-catching web. A large number of genes encode neurotoxins and there is evidence that the majority are highly selective for invertebrates. Comparison between spider species reveals a correlation between spider neurotoxin selectivity for target organisms and spider prosoma size, suggesting a possible coevolution of these two features. The genome data provides valuable insights into the biology of *P. pseudoannulata* and its potential role as a natural enemy in pest control.

Keywords: *Pardosa pseudoannulata*; wandering spider; genome; spidroin; venom; neurotoxin

Introduction

Spiders are an important group of arthropods with diverse biological and behavioural characteristics, as is illustrated by their use of both silk and venom to incapacitate prey. Some species of spider build webs for a variety of biological functions, but most notably, for the capture of prey [1]. In contrast, other species, including the pond wolf spider, *Pardosa pseudoannulata*, have a wandering lifestyle and employ venom for predation and defence (Fig. 1a). The increasing availability of spider genomic and transcriptomic data is helping to provide a better understanding of their biological and evolutionary importance [2]. In-depth genome sequencing has been reported previously for three Araneoidea spider species that produce prey-catching webs: the velvet spider *Stegodyphus mimosarum* [3] and *Stegodyphus dumicola* [4], the common house spider *Parasteatoda tepidariorum* [5,6] and the golden-orb weaver *Nephila clavipes* [7]. This has helped to provide information on evolutionary relationships and insights into phenomena such as the diversity of genes that are involved in the production of silk proteins and venom. However, despite the importance and diversity of wandering spiders, only a draft genome has been reported (with 40% coverage) for a sit-and-wait spider (*Acanthoscurria geniculate*, a cave-living species) [3].

Here, we report the first high-quality genome sequencing of a wandering spider, the pond wolf spider, *Pardosa pseudoannulata*, which belongs to the retrolateral tibial apophysis (RTA) clade of Araneomorphae. An important motivation for undertaking this project was that this would enable a comparison between the genomes of web-building and wandering species, thereby providing insights into their adaptation to differing lifestyles. In addition, *P. pseudoannulata* are predators to a range of insect pests that are of agricultural importance and, as a consequence, *P. pseudoannulata* has been identified as a possible biological control agent. The complete genome

sequencing of *P. pseudoannulata* provides a wealth of valuable information, particularly concerning its potential use for insect pest control in integrated pest management.

Results

High quality genomic DNA was extracted from *P.pseudoannulata* adults for sequencing via Illumina and PacBio technologies. Short-insert (250 bp and 350 bp) paired-end libraries, large-insert (2 kb, 5 kb, 10 kb, 15 kb and 20 kb) mate-pair libraries and 10X Genomics linked-read library were sequenced on the Illumina platform and generated 1771.69 Gb raw data (404.03 x coverage). SMRTbell libraries were sequenced on PacBio Sequel platform and generated 87.37 Gb raw data (19.92 x coverage) (Table S1). Raw data and subreads were filtered. The genome size was estimated via k-mer frequency distribution to be ~4.39 Gb (Table S2). Transcriptome sequencing of four pairs of legs, pedipalp, chelicerae, brain, venom gland, fat body, male silk gland and female silk gland was performed and each generated ~7 Gb raw data (Table S3). A draft genome of 4.27 Gb was eventually assembled with a contig N50 of 22.82 kb and scaffold N50 of 699.15 kb (Table 1, Table S4) with GC content counting for 31.36% (Table S5). The reliability and completeness of the genome assembly were evaluated with EST, CEGMA and BUSCO, with 98.79% of the raw sequence reads aligned to the assembly (Table S6), 84.63% mapped to the genome assembly and 76.71% fully covered by one scaffold with more than 90% of the transcripts mapped to one scaffold (Table S7), 91.53% of conserved eukaryotic genes found (Table S8), and 93.7% of the BUSCO dataset identified in the genome assembly (Table S9).

Genome statistics and phylogenomics

The assembled genome was ~4.26 Gb with a contig N50 of 22.82 kb and scaffold N50 of 699.15 kb (Table 1). The repeat sequences accounted for ~51.40% of the *P. pseudoannulata* genome and DNA transposons (33.46% of the genome) formed the most abundant category among the TEs, followed by long interspersed elements (LINEs, 3.34%) (Table S10, S11). The gene set contained 23,310 genes, of which 98.8% were supported by homologous evidences or transcriptomic data (Fig S1, Table S12, S13). 19,602 protein-coding genes (accounting for 92.0% of the 21,310 genes) were annotated with at least one public database (Table S14). It was notable that *P. pseudoannulata* genes were generally composed of short exons and long introns, a typical structural feature for Arachnid genes [3] (Table S12, S14).

Table 1. Summary of the *P. pseudoannulata* genome sequence data

Total sequencing data	1,859.06 Gb
Sequence coverage	423.95 x
Estimated genome size	4.42 Gb
Assembled genome size	4.26 Gb
Repeat content	51.39%
GC content	31.36%
Number of contigs	1,242,313
N50 contig size	22.82 kb
Largest contig	650 kb
Number of scaffolds	1,041,65
N50 scaffold size	699.15 kb
Largest scaffold	8,106.74 kb
Number of protein-coding genes	21,310

Annotated gene number	19,602
Average exon length	179.39 bp
Average intron length	4,132.1 bp

The phylogenetic relationship of *P. pseudoannulata* with 17 other selected species (Table S15) was analysed using 190 single-copy gene families. According to the phylogenetic analysis, *P. pseudoannulata* diverged from the common ancestral of *S. mimosarum* approximately 135.9 million years ago (MYA) and the lineage of *P. tepidariorum* and *N. clavipes* diverged from the lineage leading to *P. pseudoannulata* and *S. mimosarum* ~159 MYA (Fig. 1b, Fig. S2). The placing of spiders, ticks, scorpions and mites supported the polyphyletic nature of the Acari [3,8].

Gene family expansion

In *P. pseudoannulata* genome, 11 gene families showed significant expansion and 23 gene families showed significant contraction (Fig. 1b). Enrichment of GO terms and KEGG for *P. pseudoannulata* expanded families were performed with the EnrichPipeline [9]. A false discovery rate (FDR) threshold of 0.05 was used to define GO terms and KEGG that were significantly enriched. Predominantly enriched functional categories for these genes contained several metabolic processes and ion binding that may be related to the environmental adaptation for *P. pseudoannulata* (Table S16, S17).

Spidroin gene and silk gland

P. pseudoannulata typically hunt small insects via wandering in the field rather than building prey-catching webs. Therefore, it is of interest to compare the diversity of spidron genes in a wandering spider compared to that in web waver spiders. In total, sixteen *P. pseudoannulata* putative spidroin genes were obtained and spidroins were

classified based on their sequence homology to *N. clavipes* spidroins (Fig. 2a, Table S18). Twelve spidroin genes were designated into five spidroin types as the major ampullate (MaSp, 6), minor ampullate (MiSp, 1), aciniform (AcSp, 3), piriform (PiSp, 1) and tubuliform (TuSp, 1) spidroins based on the sequence alignment of the N-terminal domains with those of *N. clavipes*. The other 4 genes were designated as spidron (Sp) due to lack of clear evidence in sequence similarity (Fig. S3, S4). Up to 28 spidrons were catalogued into 7 spidroin types in *N. clavipes* [7] and 19 putative spidroin genes were annotated in *S. mimosarum* genome [3]. The *P. psueodannulata* spidoin gene repertoire lacked the flagelliform and aggregate spidrons, but this was not surprising given that they mainly function in prey-catching webs [1,10-14]. The fifteen complete spidroin proteins ranged from 573 (AcSp_2727) to 1977 (MaSp_2831) amino acid residues. Typically, these genes contained only one or two exons but up to 12 exons were also present (e.g. Sp_48488). The spidroins all contained the canonical structure of the repeat region (R) flanked by the relatively conserved N-terminal domain (N) and the C-terminal domain (C) (Fig. 2a, Table S18).

Dissection of adult male and female *P. pseudoannulata* identified only four types of silk glands: the major ampullate gland (Ma), minor ampullate gland (Mi), aciniform gland (Ac) and piriform gland (Pi), which were morphologically similar to the reported black widow spider silk glands (Fig. 2b) [15,16]. Typically seven types of silk glands are present in orb-weaver spiders [7] and the three absent silk gland types in *P. psuedoannulata* were the tubuliform glands, flagelliform glands and aggregate glands. The observed differences in spidroin genes, spidroin types and silk gland types between *P. pseudoannulat*a and web-weaver spiders support the conclusion that silk gland types and silk proteins are specialized in tasks involved in a variety of

biological activities [17,18]. However, whether the spidroin genes were lost in wandering spiders or expanded and differenciated in web-weavers requires further investigation.

The relative expression of the 16 spidroin genes in female and male *P. pseudoannulata* were quantified. Generally, most spidroin genes were expressed at higher levels in males than in females, however, TuSp_4038 and Sp_48488 were expressed at higher levels in females (Fig. 2c, Table S20). These differences in spidroin expression presumably reflected differences in the requirement for spidroins in each gender. For example, TuSp, which was highly expressed in females, is considered to be the most important component of egg cases [19-22]. In contrast, PiSp, which was highly expressed in males, may contribute to the silk threads used to attach to substrates [23,24]. It is also of interest to note that both MaSp and MiSp were abundantly expressed in male *P. psuedoannulata*. Further investigation of the employment of spidroins in male spiders is of interest because, to date, spidroins have been mainly studied in female spiders.

Venom toxin

Spider venom consists of numerous diverse components, however, in the present study we have focused on the best studied neurotoxins. Spider neurotoxins are peptides that contain 6-14 cysteine residues forming disulphide bridges and typically comprise the inhibitor cysteine knot (ICK) motif [25]. Thirty-two putative neurotoxin precursor genes have been identified from the venom gland transcriptome and genome analysis, forming six distinct families [26]. The neurotoxin genes of similar sequence often cluster on the same scaffold (Table S21). Other venom components have also been annotated, including venom allergen 5, hyaluronidase, astacin-like metalloprotease toxins, and Kunitz-type protease inhibitors (Table S22).

To date, at least 260 spider neurotoxins acting on ion channels have been documented in the spider toxin database ArachnoServer 3.0 [27,28]. With the aim of identifying the possible targets of *P. paseudoannulata* neurotoxins, we conducted a phylogenetic analysis with 29 *P. pseudoannulata* neurotoxins and 48 neurotoxins with known molecular targets from 14 other spider species (Fig. 3a). Further, *P. pseudoannulata* neurotoxins are clustered into groups with neurotoxins that target invertebrates only (15/29), vertebrates only (2/29) and both invertebrates and vertebrates (7/29) according to the documented neurotoxins with known selectivity (designated as reference neurotoxins in Fig. 3a). In addition, a single cluster was identified with no similarity to known neurotoxins (5/29) (Fig. 3a). We expressed one of these neurotoxins U1-lycotoxin-Pp1b *in vitro* and studied its toxicity [29]. The recombinant U1-lycotoxin-Pp1b did not show significant toxicity to mice at a dose of 10 mg/kg [30] but was found to be toxic to the insect *Nilaparvata lugens*, a typical prey of *P. pseudoannulata*, with an LD_{50} (medium lethal dose) of 1.874 nmol/g insect (13.70 mg/kg insect) (Fig. S5). Therefore, we classified the five unclustered neurotoxins into the group 'toxic to invertebrates', based on the observed selectivity of U1-lycotoxin-Pp1b (Fig. 3b, Table S23). While neurotoxins targeting invertebrates account for 69% (20/29) of genes, their proportion in terms of the transcription level is 93% (Fig. 3c, Table S23). Therefore, *P. pseudoannulata* neurotoxins have high selectivity for insects, consistent with its role as a predator of agricultural insect pests.

Spiders of different body sizes capture prey ranging from small insects to large rodents [31]. Neurotoxins from *P. psuedoannulata* and 10 other spider species were categorized by their target species as being 'invertebrate only', 'vertebrate only' or both. Information was retrieved for spider species that have at least 10 neurotoxins with identified targets documented in ArachnoSever 3.0. A clear negative correlation

was observed between the percentage of neurotoxins targeting invertebrate only (TX_inv.) and the prosoma length of a spider (liner regression, $F_{1,9} = 10.17$, $P = 0.011$, Percentage of TX_inv.=-2.96 × prosoma length + 89.23, R^2=0.5304, Fig. 3d, Fig. S6). A correlation between the size of a spider and its prey is likely to be associated with energy and nutritional requirement [32]. It seems likely that spider neurotoxins have coevolved with spider body size with a shift in prey from smaller invertebrates to larger vertebrates.

Toxins showed considerable diversity in the four species of spiders for which genome sequence data are available (Fig. 3e, Table S24). The annotated toxins can be grouped based on their structural domains. Neurotoxic Knottin toxins comprised nearly half of the toxins in *P. pseudoannulata* and their gene number exceeded that in the three web-weavers. The remarkable abundance of Knottin in *P. pseudoannulata* is consistent with the fact that wandering spiders use venom as their main strategy of predation and defence, whereas orb-weaver spiders rely more on low molecular mass compounds and behavioural adaptations (such as prey-catching webs and sticky glue) [31].

Material and Methods

Genome sequencing

Sample preparation and sequencing

For genome sequencing, three batches of *P. pseudoannulata* adults were collected from spiders reared from two individual egg cases (batch #1 of 40 adults from egg case #1; batch #2 of 60 1st-instar spiderlings from egg case #2; and batch #3 of 15 5th-instar spiderlings from egg case #2). The two egg cases were derived from two females collected at different time points from the same field in Jiangsu (λ 118.638551, φ 32.030345), China.

High quality genomic DNA was extracted using the conventional phenol/chloroform extraction protocol [33] and broken into random fragments for whole-genome shotgun sequencing. The genomic DNA was quality-examined with agarose gel electrophoresis and quantified with Qubit™ system. Short-insert (250 bp and 350 bp) paired-end libraries and large-insert (2 kb, 5 kb, 10 kb, 15 kb and 20 kb) mate-pair libraries were prepared using the standard Illumina protocols. All libraries were sequenced on the Illumina HiSeq 2000 platform with paired-end 150 bp and a total of 1,306.48 Gb sequencing data were produced. To promote genome assembly, the technologies of Pacifc Bioscience's (PacBio's) single-molecule real-time (SMRT) sequencing and 10x Genomics link-reads were also applied. For PacBio data, SMRTbell libraries were prepared using 20-kb preparation protocols and sequenced on PacBio Sequel platform, which generated 87.37 Gb (19.92x coverage) sequencing data. The 10X Genomics linked-read library was constructed and sequenced on Illumina Hiseq X Ten platform, which generated 465.21 Gb (106.09x coverage) raw reads. For Illunima sequencing, raw data were filtered according to the following criteria: reads containing adapter sequences; reads with >= 10% unidentified nucleotides (N); reads with low-quality bases (Q-value<5) more than 20%; duplicated reads generated by PCR amplification during library construction. For PacBio sequencing, subreads were filtered with the default parameters. All sequence data were summarized in Table S1.

Estimation of genome size

Genome size was estimated by analysing the k-mer frequency. The distribution of k-mer values depends on the genome characteristic and follows a Poisson distribution [34]. A total of 263 Gb high-quality short-insert reads (350 bp) were used to calculate the 17-mer frequency distribution and then estimate the *P. pseudoannulata* genome size

using the following formula [35]: genome size = (total number of 17-mers)/(position of peak depth).

Transcriptome preparation and sequencing

A batch of adult spiders were collected randomly from a field in Jiangsu (λ 118.638551, φ 32.030345), China. Tissue samples were dissected from these adults as four pairs of legs, pedipalp, chelicerae, brain, venom gland, fat body, male silk gland and female silk gland. Total RNA for each sample was extracted with TRIZOL Reagent (Thermo Fisher Scientific, Waltham, MA, USA). The concentration and purity of the RNA sample was assessed by Nanodrop spectrophotometer (Thermo Fisher Scientific, Waltham, MA, USA) and the integrity was checked by 2100 Bioanalyzer (Agilent, USA). RNA sequencing (RNA-seq) libraries were constructed using the NEBNext® mRNA Library Prep Master Mix Set for Illumina® (New England Biolab, RRID: SCR_013517) according to the manufacturer's instructions. All libraries were sequenced on the Illumina Hiseq X Ten with paired-end 150 bp. Information for all RNA-seq data was summarized in Table S3.

Genome assembly

For genome assembly of *P. pseudoannulata*, Platanus (PLATform for Assembling Nucleotide Sequences, RRID: SCR_015531) (version 1.2.4) [36] was first used to construct the genome assembly backbone with all Illumina reads. Briefly, Platanus carried out following three steps: (1) all short-insert paired-end reads were used to construct *de Bruijn* graphs with automatically optimized k-mer sizes; (2) all short-insert paired-end reads and large-insert mate-pair reads were aligned to the contigs for scaffolding; (3) paired-end reads were aligned to scaffolds to close the gap. Then GapCloser (RRID: SCR_015026) (version 1.12) [37] was used to fill the gaps in intra-scaffold. Subsequently, the PacBio data were used to fill additional gaps with the

252 software PBJelly (RRID: SCR_012091) (version 1.3.1) [38] with default parameters.
253 After that, the resulting scaffolds were further connected to super-scaffolds using the
254 10X Genomics linked-reads by the software fragScaff (version 140324.1) [39]
255 The completeness of the genome assembly and the uniformity of the sequencing were
256 evaluated with several approaches. Briefly, BWA (Burrows-Wheeler Aligner, RRID:
257 SCR_010910) [40] was used to align high-quality short-insert reads onto the *P.*
258 *pseudoannulata* genome with parameters of '-k 32 -w 10 -B 3 -O 11 -E 4'. Gene
259 region completeness was evaluated with the transcripts assembled by Trinity (version
260 2.1.1) [41]. All assembled transcript (length >= 200bp) were align onto the genome by
261 the software BLAT (BLAT, RRID: SCR_011919) [36] with default parameters.
262 CEGMA (Core Eukaryotic Genes Mapping Approach, RRID: SCR_015055) [42] was
263 used to identify the exon-intron structures. Further, BUSCO (Benchmarking
264 Universal Single Copy Orthologs, RRID: SCR_015008) (v3.0.2) [43] was used to assess
265 the genome completeness with a set of 1066 arthropoda single-copy orthologous
266 genes.

267 **Genome annotation**

268 **Repetitive element identification**

269 Transposable elements (TEs) were identified with homology alignment and *de novo*
270 prediction. A *de novo* repeat library was built using RepeatModeler (RRID:
271 SCR_015027) (version 1.0.4) [44,45], RepeatScout (RRID: SCR_014653) (version 1.0.5)
272 [46], and LTR_FINDER (RRID: SCR_015247) (version 1.06) [47] with default parameters.
273 Known TEs were idenfied via homology-based prediction using the RepeatMasker
274 (RRID: SCR_012954) (version 4.0.5) [44] with default parameters against the RepBase
275 library [48,49].In addition, tandem repeats were identified using Tandem Repeats Finder

(RRID: SCR_005659) [50,51] with parameters "Match=2, Mismatch=7, Delta=7, PM=80, PI=10, Minscore=50, MaxPeriod=2000".

Protein-coding gene prediction

Protein-coding genes were predicted with a combination of homology-based prediction, *de novo* prediction, and transcriptome sequencing-based prediction methods. For the homology-based gene prediction, protein sequences from four species including *Stegodyphus mimosarum, Parasteatoda tepidariorum, Tetranychus urticae* and *Drosophila serrata* [52] were aligned to our assembled genome using TBLASTN (RRID: SCR_011822) [53,54] with e-value <=1e-5. The BLAST hits were conjoined with the software Solar [55]. Then GeneWise (RRID: SCR_015054) (version 2.2.0) [56,57] was applied to predict gene models based on the alignment sequences. The *de novo* prediction was performed using Augustus (RRID: SCR_008417) (version 3.0.2) [58,59], GeneScan (RRID: SCR_012902) (version 1.0) [60,61], GeneID (version 1.4) [62,63], GlimmerHMM (RRID: SCR_002654) (version 3.0.4) [64,65] and SNAP (Semi-HMM-based Nucleioc acid Parser, RRID: SCR_007936) [66,67] on the repeat-masked genome. For the transcriptome-based prediction, RNA-Seq data from different tissues including four pairs of legs, pedipalp, chelicerae, brain, venom gland and fat body were aligned to the *P. pseudoannulata* genome using TopHat (RRID: SCR_013035) (version 2.0.13) [68,69] and gene strutures were predicted with Cufflinks (RRID: SCR_014597) (version 2.1.1) [70,71]. In addition, the RNA-Seq data was assembled by Trinity (RRID: SCR_013048) (version 2.1.1) [41,72]. These assembled sequences were aligned against our assembled genome by PASA (Program to Assemble Spliced Alignment, RRID: SCR_014656) [73,74] and generated gene models were used as the training set for the softwares Augustus, GlimmerHMM and SNAP (Semi-HMM-based Nucleic Acid Parser, RRID: SCR_002127) [67]. Eventually, gene models

obtained from all the methods were integrated into a comprehensive and non-redundant gene set with the software EVidenceModeler (EVM, RRID: SCR_014659) [75,76].

Functional annotation

To obtain functional annotation, all predicted protein-coding sequences in *P. pseudoannulata* genome were aligned to public databases including National Center for Biotechnology Information nonredundant protein (NR) [77] and SwissProt [78,79]. The known motifs and domains were annotated by searching InterPro databases [80] including Pfam (RRID: SCR_004726) (version 27.0) [81,82], PRINTS (RRID: SCR_003412) (version 42.0) [83,84], PROSITE (RRID: SCR_003457) (version 20.89) [85,86], ProDom (RRID: SCR_006969) (version 2006.1) [87,88], SMART (RRID: SCR_005026) (version 6.2) [89,90] and PANTHER (RRID: SCR_004869) (version 7.2) [91,92] with the software InterProScan (RRID: SCR_005829) (version 4.7) [80,93]. Gene Ontology (GO, RRID: SCR_002811) [94,95] terms for each gene were obtained from the corresponding InterPro entry. Kyoto Encyclopedia of Genes and Genomes (KEGG, RRID: SCR_012773) databases [96,97] were searched to identify the pathways in which the genes might be involved.

Phylogeny and divergence time estimation

Gene family analysis was performed with 18 species including *Caenorhabditis elegans*, *Drosophila melanogaster*, *Apis mellifera*, *Tribolium castaneum*, *Nilaparvata lugens*, *Acyrthosiphon pisum*, *Bombyx mori*, *Hyalella Azteca*, *Daphnia magna*, *Eurytemora affinis*, *Tetranychus urticae*, *Ixodes scapularis*, *Metaseiulus occidentalis*, *Centruroides sculpturatus*, *Stegodyphus mimosarum*, *Parasteatoda tepidariorum*, *Nephila clavipes*, and *P. pseudoannulata* (Table S15). Only the longest transcript of a gene was retained as the representative if the gene had alternative splicing isoforms

identified. Genes with protein sequences shorter than 30 amino acids were removed. Then, the similarities between genes in all selected genomes were identified using all-versus-all BLASP with an E-value threshold of 1e-7 and all the blast hits were concatenated by the software Solar [55]. Finally, gene families were constructed using OrthoMCL [98,99] with the setting of "-inflation 1.5". In total, the protein-coding genes were clustered into 29,995 gene families and 190 single-copy orthologs.

The phylogenetic relationship of *P. pseudoannulata* with the other 17 selected species was analysed using the 190 single-copy gene families. Protein sequences of the ortholog genes were aligned using the multiple alignment software MUSCLE with default parameters [100]. Then the alignments of each family were concatenated into a super alignment matrix and RAxML (version 8.0.19) [101,102] was used to reconstruct the phylogenetic tree through maximum likelihood methods with default substitution model-PROTGAMMAAUTO. Divergence times of these species were estimated using the MCMCtree program in PAML [103,104] with the parameters of 'burn-in=10000, sample-number=100,000 and sample-frequency=2'. Calibration points applied in present study were obtained from the TimeTree database (*Drosophila melanogaster*, *Bombyx mori*, *Tribolium castaneum*, *Apis mellifera*, 238~ 377 MYA; *Apis mellifera*, *Tribolium castaneum*, *Bombyx mori*, *Drosophila melanogaster*, *Acyrthosiphon pisum*, *Nilaparvata lugens*, 295~305 MYA; *Caenorhabditis elegans* and other species, 521~581 MYA). [105,106].

Gene family contraction and expansion

Expansion and contraction analysis of orthologous gene families was performed using CAFÉ program (version 2.1) (Computational Analysis of gene Family Evolution, RRID: SCR_005983) [107,108]. The program uses a random birth and death model to infer changes of gene families along each lineage of phylogenetic tree. Based on a

probabilistic graphical model, this method calculates a p-value for transitions between parent and child nodes gene family size over a phylogeny. The gene families were significantly expanded or contracted in the *P. pseudoannulata* genome with a p-value of 0.05.

Spidroin gene classification and quantification

Multiple rounds of BLAST (RRID: SCR_004870) were run in the genome database to identify putative spidroin genes. The spidroin genes in *N. clavipes* [7] and *S. mimosarum* [3] were first used as queries for BLAST and the resultant *P. pseudoannulata* spidroin genes were then added into the query repertoire to run further BLAST searches [7]. The scaffolds containing the putative spidroin genes were then subjected to Augustus (RRID: SCR_008417) [109] for gene prediction and the predicted spidroin genes were manually checked for the presence of structural feature, namely, the N-terminal domain, the repeat region and the C-terminal domain. The manually checked spidroin genes were then examined by BLAST in the silk gland transcriptomes of both males and females for their corresponding transcripts. Spidroin genes were confirmed if at least one transcript aligned with 95% identity. The N-terminal domain (130 amino acids) of the spidroins in *P. pseudoannulata* and *N. clavipes* were aligned with ClustalW function and a phylogenetic tree was constructed with maximum-likelihood method (1000 replicates) in MEGA (RRID: SCR_000667, version 7) [110] (Fig. S3, S4). Gene structures were drawn to scale in IBS (version 1.0.3) [111].

Silk glands were dissected and identified following protocols relating to the western black widow spider [15,16]. Images were obtained with a portable video microscope (3R-MSA600, Anyty, 3R Eddyteck Corp., China) and contrasted with Photoshop CS6.

Spider adults were collected from the paddy fields in Nanjing (Jiangsu, China), and reared in laboratory conditions for at least two weeks. Spiders were anesthetized with CO_2 and silk glands were carefully collected. The entire silk glands from 10 females and 15 males were pooled as one sample, respectively. Three samples were prepared for each gender. Each sample was kept in 200 μL RNA*later* (Thermo Fisher Scientific, Waltham, MA, USA) at -80 °C until total RNA extraction.

Total RNA was extracted from silk gland samples with GeneJET RNA Purification Kit (Thermo Fisher Scientific, Waltham, MA, USA) after removing the RNA*later* and eluted with 44 μL nuclease-free water. Genomic DNA was removed with TURBO DNA-*free* Kit (Thermo Fisher Scientific, RRID:SCR_008452) following the manufacturer's instructions. The quality and quantity of the total RNAs were monitored with NanoDrop spectrophotometer (Thermo Fisher Scientific) and 2% agarose gel electrophoresis. RNA samples were stored at -80 °C. cDNA was synthesized with 2 μg RNA using PrimeScript RT Reagent Kit (TaKaRa, Kyoto, Japan) and then stored at -20 °C. Primers for quantitative real-time PCR (qPCR) were designed using Beacon Designer (version 7.92, PREMIER Biosoft International, CA, USA) (Table S19). Two pairs of universal primers were designed for MaSp (MaSp_691565, MaSp_3359, MaSp_4789, MaSp_258724, MaSp_2831) and AcSp (AcSp_1925.1, AcSp_1925.2), respectively, due to the high similarity of their sequences. Glyceraldehyde-3-phosphatedehydrogenase (GAPDH) and elongation factor 1-alpha (EF1α) genes were selected as the reference genes for spidroin gene quantification. The specificity and efficiency of the primers were validated via standard curves with five serial cDNA dilutions and the melt curve with a temperature range 60-95 °C. qPCR was performed using SYBR Premix Ex Taq Kit (TaKaRa, Kyoto, Japan) following the manufacturer's instructions on a 7500 Real-Time PCR

System (Applied Biosystems, RRID:SCR_005039). Reagents were assembled in a 20 µL reaction containing 10 µL SYBR Premix Ex Taq, 6.8 µL sterile water, 0.4 µL forward primer, 0.4 µL reverse primer, 0.4 µL ROX Reference Dye II and 2 µL cDNA. The reaction program was 95 °C for 30 sec, 40 cycles of 95 °C for 5 sec and 60 °C for 34 sec. No template control (NTC) and no reverse transcriptase control (NRT) were included as negative controls to eliminate the possibilities of reagent contamination and genomic DNA contamination. Each reaction was performed in two technical replicates and three biological samples were tested. Ct values of qPCR were exported from 7500 Real-Time PCR Software (RRID:SCR_014596) (version 2.0.6). The expression levels of target genes were relative to the geometric mean of two reference genes [112] following the $2^{-\Delta CT}$ method [113]. Statistical analyses were performed with GraphPad Prism (RRID: SCR_002798) (version 7).

Neurotoxin identification and bioassay

Identification of neurotoxin genes and comparative analysis among spiders

Neurotoxin candidates were retrieved via BLAST in the genome database with neurotoxins from ArachnoServer 3.0 as queries [27,28]. They were identified as neurotoxins when the proteins met the criteria such as containing 6-14 cysteine residues and the canonical neurotoxin domains. The neurotoxins were characterized with their signal peptide via SignalP 4.1 Server [114,115], propeptide, and the Cys-Cys disulfide bridge pattern. Inhibitor Cystine Knots (ICK) were predicted on the KNOTTIN database[116]. Toxin genes subjected to interspecific comparison were retrieved from the genome annotation with astacin-like metalloprotease toxin excluded. Non-Knottin toxins were subjected to NCBI domain analysis and grouped accordingly, putative neurotoxins with Spider_toxin or toxin_35 domain, cysteine protease inhibitors containing TY (thyroglobulin type I repeats, accession no.

cd00191), serine protease inhibitors containing KU (BPTI/Kunitz family of serine protease inhibitors, accession no. cd00109), Trypsin-like serine proteases with Tryp_SPc (Trypsin-like serine protease, accession no. cd00190), SVWC family proteins containing SVWC (single-domain von Willebrand factor type C proteins, accession no. pfam15430), colipases with COLIPASE (Colipases, accession no. smart00023) and the rest designated as other toxins.

Construction of neurotoxin expression vector

The open reading frame of neurotoxin U1-lycotoxin-Pp1b was cloned into the prokaryotic expression vector pLicC-MBP-APETx2 [29,117]. *Kpn* I and *Ava* I were used for double digestion, and primer sequences were: cggggtaccccggaaaatctgtattttcagggcaaggcatgcaccccaaggttttac (forward) and ccctcgagggttaaccgaatagagtcttaatcttgcc (reverse). For the PCR amplification, the high-fidelity PrimerSTAR (TaKaRa, Tokyo, Japan) was used, and the amplification program was 94°C for 3 minutes, followed by 30 cycles of 94°C for 30 seconds, 55°C for 30 seconds, 72°C for 30 seconds, and finally 72°C for 10 minutes. The PCR products were gel-purified using a Gel Extraction Kit (CWBIO, Nanjing, China), ligated into sequencing vector, and sequenced at Genscript Biotechnology Co. Ltd. (Nanjing, China). Plasmid extraction was performed using Mini Plasmid Extraction Kit I (OMEGA, Guangzhou, China), and double digestion using *Kpn* I (TaKaRa, Tokyo, Japan) and *Ava* I (TaKaRa, Tokyo, Japan). After the target gene and vector were recovered, they were ligated with T4 DNA ligase (TaKaRa, Tokyo, Japan) at 4°C overnight. Subsequently, the ligation product was transformed into *Escherichia coli* BL21 strain, and sequenced at Genscript Biotechnology Co. Ltd. (Nanjing, China). A positive clone was selected and the final concentration of 40% glycerol was added for preservation at -80°C.

Expression and purification of the recombinant neurotoxin

Positive clones were cultivated in LB liquid medium containing 100 mg/L carbenicillin at 37°C in a constant temperature shaker with 250 r/min for 14h. The culture broth was inoculated in an LB liquid medium containing 100 mg/L carbenicillin at a ratio of 1:100 and cultured with 250 r/min at 37°C for 4h. IPTG was added into the culture at a final concentration of 0.5 mmol/L, 160r/min, and 25°C to induce the expression for 4h. Bacteria were collected after centrifuging at 4000rpm for 10min at 4°C and resuspended with 20mM Tris-HCl (pH 7.4). Then, 100μg/ml lysozyme, 0.1% Trition X-100, 0.5mM PMSF were added to the suspension and the digestion was performed at 37°C for 1 hour. Bacteria were then ultrasonicated and debris were removed by centrifugation with 16,000 rpm for 20min at 4°C, and the supernatant was filtered through a 0.22 μm filter.

The recombinant toxin was purified using AKTA Avant automated protein purification system (GE, Uppsala, Sweden). Initially, the fusion protein was collected by affinity chromatography using nickel column HisTrap HP (GE, Uppsala, Sweden), and then transferred to TEV protease buffer using desalting column HiPrep 26/10 Desalting (GE, Uppsala, Sweden) and digested with TEV protease (Solarbio, Beijing, China) at 16°C for 10h. Next, TEV protease buffer was replaced by PBS using the desalting column. Finally, the protein label was removed by affinity chromatography using nickel column, and the purity of recombinant toxin was detected by SDS-PAGE.

Biological activity assay of recombinant neurotoxin

The insecticidal activity of the recombinant neurotoxin against 5th-instar *Nilaparvata lugens* nymphs was determined by microinjection [118]. *N. lugens* nymphs were injected with neurotoxin solutions at a series of concentrations with 3 replicates of 20 individuals per replicate. PBS was injected as control solution. Before injection, the

476 test insects were anesthetized with CO_2 and each insect was injected with 30nl of
477 recombinant neurotoxin. After injection, the test insects were checked 1h or 12h later.
478 The toxicity of the recombinant neurotoxin against mice was measured by lateral
479 ventricle injection [119].

480 ## Discussions

481 The complete genome sequencing of the wandering spider *P. pseudoannulata*
482 provides valuable insights into the aspects of the biology of wandering spiders,
483 including diversity of spidroin genes and invertebrate-specific neurotoxins which may
484 have potential importance in developing novel pest management strategies.

485 The evolutionary diversification of spiders has long been discussed. The focus of
486 the debate has been whether the orb web origin is monophyletic or polyphyletic [1,2,120].
487 Notably, the cursorial, non-web building spider taxa from RTA clade has proven to be
488 more important than previously thought in the phylogenetic analysis with
489 morphological, behavioural and molecular evidences [2,120]. In addition to the
490 distinction in silk use, wandering spiders differs from the web weaver spiders in
491 habitat and biotic interaction, which can also promote the diversification [2]. Therefore,
492 the massive genomic information of *P. pseudoannulata* offers added value to the
493 diversification analysis. Spiders of different ecological niches have evolved their
494 corresponding behaviours and lifestyle. Genome comparison analysis of spiders of
495 different lifestyles or habitats will reveal primary hints for molecular mechanisms of
496 spiders' evolutionary adaptation.

497 The present studies were prompted, in part, an interest in the genetic basis for
498 differences in methods of predation by spiders and, in particular, in the use of
499 neurotoxins to incapacitate insect prey. Although further work will be required to
500 understand the molecular targets and mode of actions of *P. psuedoannulata*

neurotoxins, it is possible that a better understanding of spider toxins may lead to the development of novel pest control agents applicable to integrated pest management and other potential biomedical applications.

Availability of supporting data and materials

The *P. pseudoannulata* genome has been deposited in GenBank under accession No. SBLA00000000 and transcriptomes have been deposited to NCBI Sequence Read Archive under accession No. SRR8083387-SRR8083398.

Additional files

Table S1-S3. Statistics of genome and transcriptome sequencing

Table S4-S6. Genome assembly

Table S7-S9. Genome evaluation

Table S10-S14. Genome annotation

Table S15-S17. Comparative genomes, gene expansion and contraction

Table S18-S20. Spidroin gene classification and quantification

Table S21-S24. Venom components and neurotoxins

Figure S1. Venndiagram of gene sets obtained using three prediction methods (*de novo*, homology-based, RNAseq-based).

Figure S2. Estimation of divergence time.

Figure S3. Phylogenetic tree of 16 *P. pseudoannulata* spidroins.

Figure S4. Phylogenetic tree of 16 *P. pseudoannulata* spidroins and 26 complete *N. clavipes* spidrions.

Figure S5. Toxicity assay of the recombinant neurotoxin U1-lycotoxin-Pp1.

Figure S6. Linear regression analysis of spider prosoma length and the number of neurotoxins targeting invertebrate prey species.

Abbreviations

Ac: aciniform; bp: base pair; BUSCO: benchmarking universal single-copy orthologs; BWA: Burrows-Wheeler Alignment tool; CDS: coding sequence; CEGMA: core eukaryotic genes mapping approach; EF1α: elongation factor 1-alpha; EST: expressed sequence tag; FDR: false discovery rate; FPKM: Fragments Per Kilobase of exon model per Million mapped fragments; GAPDH: glyceraldehyde-3-phosphatedehydrogenase ; Gb: gigabases; GO: Gene Ontology ; KEGG: Kyoto Encyclopedia of Genes and Genomes ; Ma: major ampullate ; Mi: minor ampullate ; MYA: million years ago; NJ: neighbour joining; NRT: no reverse transcriptase control; NTC: no template control; Pi: piriform; RTA: retrolateral tibial apophysis; Sp: spidroin; TE: transposable element; Tu: tubuliform.

Animal care

Animal experimental procedures were approved by the Laboratory Animal Ethical Committee of Nanjing Agricultural University (No. PZ2019021) and performed accordingly.

Competing interests

The authors declare that they have no competing interests.

Authors' contributions

Z. Liu initiated and supervised the project. H. Bao and Y. Yang contributed to the sample collection and handling. M. Liu performed genome sequencing, assembly and primary annotation. M. Liu, J. Li and H. Gao performed the comparative genomic analysis. N. Yu, Y. Zhang, H. Bao, T. Van Leeuwen, N. S. Millar and Z. Liu contributed to the data mining and analysis. N. Yu and Z. Yang conducted the analysis and experimental validation of spidroin genes. L. Huang and Z. Wang

549 performed the analysis and experimental validation of neurotoxins. N. Yu and J. Li
550 submitted data to NCBI. N. Yu and Z. Liu wrote the initial draft of the manuscript. N.
551 Yu, T. Van Leeuwen, N. Millar and Z. Liu revised the manuscript. All authors have
552 read and approved the final manuscript.

553 These authors contributed equally: Na Yu, Jingjing Li and Meng Liu.

554 **Current address:**

555 Yuanxue Yang, Cotton Research Center, Shandong Academy of Agricultural
556 Sciences, Jinan 250100, China

557 Acknowledgments

558 We thank Dr. Huixing Lin (MOE joint international research laboratory of animal
559 health and food safety, Nanjing Agricultural University) for the neurotoxin assay with
560 mice. The work was supported by National Natural Science Foundation of China
561 (grant number 31772185, 31601656, 31701823).

562 References

563 1. Blackledge, T.A. *et al.* Reconstructing web evolution and spider diversification in
564 the molecular era. *Proceedings of the National Academy of Sciences of the United*
565 *States of America* **106**, 5229-5234 (2009).
566 2. Fernandez, R. *et al.* Phylogenomics, diversification dynamics, and comparative
567 transcriptomics across the spider tree of life. *Current Biology* **28**, 2190-2193
568 (2018).
569 3. Sanggaard, K.W. *et al.* Spider genomes provide insight into composition and
570 evolution of venom and silk. *Nature Communications* **5** (2014).
571 4. Liu, S., Aagaard, A., Bechsgaard, J. & Bilde, T. DNA methylation patterns in the
572 social spider, *Stegodyphus dumicola*. *Genes* **10** (2019).
573 5. Gendreau, K.L. *et al.* House spider genome uncovers evolutionary shifts in the
574 diversity and expression of black widow venom proteins associated with extreme
575 toxicity. *BMC Genomics* **18**, 178 (2017).

6. Schwager, E.E. *et al.* The house spider genome reveals an ancient whole-genome duplication during arachnid evolution. *BMC Biology* **15** (2017).
7. Babb, P.L. *et al.* The Nephila clavipes genome highlights the diversity of spider silk genes and their complex expression. *Nature Genetics* **49**, 895-903 (2017).
8. Regier, J.C. *et al.* Arthropod relationships revealed by phylogenomic analysis of nuclear protein-coding sequences. *Nature* **463**, 1079-1083 (2010).
9. Chen, S. *et al. De novo* analysis of transcriptome dynamics in the migratory locust during the development of phase traits. *Plos One* **5** (2010).
10. Adrianos, S.L. *et al. Nephila clavipes* flagelliform silk-like GGX motifs contribute to extensibility and spacer motifs contribute to strength in synthetic spider silk fibers. *Biomacromolecules* **14**, 1751-1760 (2013).
11. Hayashi, C.Y. & Lewis, R.V. Molecular architecture and evolution of a modular spider silk protein gene. *Science* **287**, 1477-1479 (2000).
12. Choresh, O., Bayarmagnai, B. & Lewis, R.V. Spider web glue: two proteins expressed from opposite strands of the same DNA sequence. *Biomacromolecules* **10**, 2852-2856 (2009).
13. Jain, D., Amarpuri, G., Fitch, J., Blackledge, T.A. & Dhinojwala, A. Role of hygroscopic low molecular mass compounds in humidity responsive adhesion of spider's capture silk. *Biomacromolecules* **19**, 3048-3057 (2018).
14. Singla, S., Amarpuri, G., Dhopatkar, N., Blackledge, T.A. & Dhinojwala, A. hygroscopic compounds in spider aggregate glue remove interfacial water to maintain adhesion in humid conditions. *Nature Communications* **9**, 3048-3057 (2018).
15. Jeffery, F. *et al.* Microdissection of black widow spider silk-producing glands. *Journal of Visualized Experiments* (2011).
16. Chaw, R.C. & Hayashi, C.Y. Dissection of silk glands in the western black widow Latrodectus hesperus. *Journal of Arachnology* **46**, 159-161 (2018).
17. Vollrath, F. & Knight, D.P. Liquid crystalline spinning of spider silk. *Nature* **410**, 541-548 (2001).
18. Chaw, R.C. *et al.* Intragenic homogenization and multiple copies of prey-wrapping silk genes in Argiope garden spiders. *Bmc Evolutionary Biology* **14**(2014).

19. Casem, M.L., Collin, M.A., Ayoub, N.A. & Hayashi, C.Y. Silk gene transcripts in the developing tubuliform glands of the Western black widow, *Latrodectus hesperus*. *Journal of Arachnology* **38**, 99-103 (2010).
20. Garb, J.E. & Hayashi, C.Y. Modular evolution of egg case silk genes across orb-weaving spider superfamilies. *Proceedings of the National Academy of Sciences of the United States of America* **102**, 11379-11384 (2005).
21. Hu, X.Y. *et al.* Spider egg case core fibers: Trimeric complexes assembled from TuSp1, ECP-1, and ECP-2. *Biochemistry* **45**, 3506-3516 (2006).
22. Jiang, P. *et al.* Structure, composition and mechanical properties of the silk fibres of the egg case of the Joro spider, *Nephila clavata* (Araneae, Nephilidae). *Journal of Biosciences* **36**, 897-910 (2011).
23. Blasingame, E. *et al.* Pyriform spidroin 1, a novel member of the silk gene family that anchors dragline silk fibers in attachment discs of the black widow spider, *Latrodectus hesperus*. *Journal of Biological Chemistry* **284**, 29097-29108 (2009).
24. Geurts, P. *et al.* Synthetic spider silk fibers spun from pyriform spidroin 2, a glue silk protein discovered in orb-weaving spider attachment discs. *Biomacromolecules* **11**, 3495-3503 (2010).
25. Norton, R.S. & Pallaghy, P.K. The cystine knot structure of ion channel toxins and related polypeptides. *Toxicon* **36**, 1573-1583 (1998).
26. Huang, L., Wang, Z., Yu, N., Li, J. & Liu, Z. Toxin diversity revealed by the venom gland transcriptome of *Pardosa pseudoannulata*, a natural enemy of several insect pests. *Comparative Biochemistry and Physiology D-Genomics & Proteomics* **28**, 172-182 (2018).
27. Pineda, S.S. *et al.* ArachnoServer 3.0: an online resource for automated discovery, analysis and annotation of spider toxins. *Bioinformatics* **34**, 1074-1076 (2018).
28. ArachnoServer spider toxin database. http://www.arachnoserver.org/mainMenu.html.
29. Anangi, R., Rash, L.D., Mobli, M. & King, G.F. Functional expression in Escherichia coli of the disulfide-rich sea anemone peptide APETx2, a potent blocker of acid-sensing ion channel 3. *Marine Drugs* **10**, 1605-1618 (2012).
30. de Lima, M.E. *et al.* The toxin Tx4(6-1) from the spider Phoneutria nigriventer slows down Na+ current inactivation in insect CNS via binding to receptor site 3. *Journal of Insect Physiology* **48**, 53-61 (2002).

641 31. Kuhn-Nentwig, L., Stoecklin, R. & Nentwig, W. Venom composition and
642 strategies in spiders: Is everything possible? *Advances in Insect Physiology* **40**, 1-
643 86 (2011).
644 32. Nentwig, W. & Wissel, C. A comparison of prey lengths among spiders.
645 *Oecologia* **68**, 595-600 (1986).
646 33. Sambrook, J., Russell, D.W., Sambrook, J. & Russell, D.W. *Molecular cloning:*
647 *A laboratory manual*, (Cold Spring Harbor Laboratory Press , 10 Skyline Drive,
648 Plainview, NY, 11803-2500, USA, 2001).
649 34. Li, R. *et al.* The sequence and de novo assembly of the giant panda genome.
650 *Nature* **463**, 1106-1106 (2010).
651 35. Liu, B. *et al.* Estimation of genomic characteristics by analyzing k-mer frequency
652 in *de novo* genome projects. *Quantitative Biology* **35**, 62-67 (2013).
653 36. Kajitani, R. *et al.* Efficient de novo assembly of highly heterozygous genomes
654 from whole-genome shotgun short reads. *Genome Research* **24**, 1384-1395
655 (2014).
656 37. English, A.C. *et al.* Mind the gap: Upgrading genomes with Pacific Biosciences
657 RS long-read sequencing technology. *Plos One* **7**(2012).
658 38. English, A.C., Salerno, W.J. & Reid, J.G. PBHoney: identifying genomic variants
659 via long-read discordance and interrupted mapping. *Bmc Bioinformatics* **15**(2014).
660 39. Adey, A. *et al.* In vitro, long-range sequence information for de novo genome
661 assembly via transposase contiguity. *Genome Research* **24**, 2041-2049 (2014).
662 40. Li, H. & Durbin, R. Fast and accurate short read alignment with Burrows-
663 Wheeler transform. *Bioinformatics* **25**, 1754-1760 (2009).
664 41. Grabherr, M.G. *et al.* Full-length transcriptome assembly from RNA-Seq data
665 without a reference genome. *Nature Biotechnology* **29**, 644-652 (2011).
666 42. Parra, G., Bradnam, K. & Korf, I. CEGMA: a pipeline to accurately annotate core
667 genes in eukaryotic genomes. *Bioinformatics* **23**, 1061-1067 (2007).
668 43. Simao, F.A., Waterhouse, R.M., Ioannidis, P., Kriventseva, E.V. & Zdobnov,
669 E.M. BUSCO: assessing genome assembly and annotation completeness with
670 single-copy orthologs. *Bioinformatics* **31**, 3210-3212 (2015).
671 44. Tarailo-Graovac, M. & Chen, N. Using RepeatMasker to identify repetitive
672 elements in genomic sequences. *Current protocols in bioinformatics* **Chapter 4**,
673 Unit 4.10-Unit 4.10 (2009).
674 45. RepeatModeler. http://www.repeatmasker.org/RepeatModeler/.

675 46. Price, A.L., Jones, N.C. & Pevzner, P.A. De novo identification of repeat families
676 in large genomes. *Bioinformatics* **21**, I351-I358 (2005).
677 47. Xu, Z. & Wang, H. LTR_FINDER: an efficient tool for the prediction of full-
678 length LTR retrotransposons. *Nucleic Acids Research* **35**, W265-W268 (2007).
679 48. Bao, W., Kojima, K.K. & Kohany, O. Repbase Update, a database of repetitive
680 elements in eukaryotic genomes. *Mobile DNA* **6**(2015).
681 49. RepBase. https://www.girinst.org/server/RepBase/index.php.
682 50. Benson, G. Tandem repeats finder: a program to analyze DNA sequences.
683 *Nucleic Acids Research* **27**, 573-580 (1999).
684 51. Tandem Repeats Finder. http://tandem.bu.edu/trf/trf.download.html.
685 52. Wang, Z. *et al*. The draft genomes of soft-shell turtle and green sea turtle yield
686 insights into the development and evolution of the turtle-specific body plan.
687 *Nature Genetics* **45**, 701-706 (2013).
688 53. Altschul, S.F. *et al*. Gapped BLAST and PSI-BLAST: a new generation of
689 protein database search programs. *Nucleic Acids Research* **25**, 3389-3402 (1997).
690 54. TBLASTN. https://blast.ncbi.nlm.nih.gov/Blast.cgi.
691 55. Darriba, D., Taboada, G.L., Doallo, R. & Posada, D. jModelTest 2: more models,
692 new heuristics and parallel computing. *Nature Methods* **9**, 772-772 (2012).
693 56. Birney, E., Clamp, M. & Durbin, R. GeneWise and genomewise. *Genome*
694 *Research* **14**, 988-995 (2004).
695 57. GeneWise. https://www.ebi.ac.uk/~birney/wise2/.
696 58. Stanke, M., Schoffmann, O., Morgenstern, B. & Waack, S. Gene prediction in
697 eukaryotes with a generalized hidden Markov model that uses hints from external
698 sources. *Bmc Bioinformatics* **7**(2006).
699 59. Stanke, M. & Waack, S. Gene prediction with a hidden Markov model and a new
700 intron submodel. *Bioinformatics* **19**, II215-II225 (2003).
701 60. Salamov, A.A. & Solovyev, V.V. Ab initio gene finding in Drosophila genomic
702 DNA. *Genome Research* **10**, 516-522 (2000).
703 61. GeneScan. http://genome.dkfz-heidelberg.de/cgi-bin/GENSCAN/genscan.cgi.
704 62. Parra, G., Blanco, E. & Guigo, R. GeneID in Drosophila. *Genome Research* **10**,
705 511-515 (2000).
706 63. GeneID. http://genome.crg.es/software/geneid/index.html.

64. Majoros, W.H., Pertea, M. & Salzberg, S.L. TigrScan and GlimmerHMM: two open source ab initio eukaryotic gene-finders. *Bioinformatics* **20**, 2878-2879 (2004).
65. GlimmerHMM. http://ccb.jhu.edu/software/glimmerhmm/.
66. Korf, I. Gene finding in novel genomes. *BMC Bioinformatics* **5**(2004).
67. Semi-HMM-based Nucleic Acid Parser. http://korflab.ucdavis.edu/software.html.
68. Trapnell, C., Pachter, L. & Salzberg, S.L. TopHat: discovering splice junctions with RNA-Seq. *Bioinformatics* **25**, 1105-1111 (2009).
69. TopHat. https://ccb.jhu.edu/software/tophat/index.shtml.
70. Trapnell, C. *et al.* Transcript assembly and quantification by RNA-Seq reveals unannotated transcripts and isoform switching during cell differentiation. *Nature Biotechnology* **28**, 511-515 (2010).
71. Cufflinks. http://cole-trapnell-lab.github.io/cufflinks/.
72. Trinity. https://github.com/trinityrnaseq/trinityrnaseq/wiki.
73. Haas, B.J. *et al.* Improving the Arabidopsis genome annotation using maximal transcript alignment assemblies. *Nucleic Acids Research* **31**, 5654-5666 (2003).
74. Program to Assemble Spliced Alignments. https://github.com/PASApipeline/PASApipeline/wiki.
75. Haas, B.J. *et al.* Automated eukaryotic gene structure annotation using EVidenceModeler and the program to assemble spliced alignments. *Genome Biology* **9** (2008).
76. EVidenceModeler. https://github.com/EVidenceModeler/EVidenceModeler/.
77. National Center for Biotechnology Information. https://www.ncbi.nlm.nih.gov/protein/.
78. Bairoch, A. & Apweiler, R. The SWISS-PROT protein sequence database and its supplement TrEMBL in 2000. *Nucleic Acids Research* **28**, 45-48 (2000).
79. UniProtKB. http://www.uniprot.org/uniprot/.
80. Mulder, N. & Apweiler, R. InterPro and InterProScan: tools for protein sequence classification and comparison. in *Comparative Genomics* (ed. Bergman, N.H.) 59-70 (Humana Press, Totowa, NJ, 2007).
81. Bateman, A. *et al.* The Pfam protein families database. *Nucleic Acids Research* **28**, 263-266 (2000).
82. Pfam. http://pfam.xfam.org/.

740 83. Attwood, T.K., Beck, M.E., Bleasby, A.J. & Parrysmith, D.J. PRINTS - a
741 database of protein motif fingerprints. *Nucleic Acids Research* **22**, 3590-3596
742 (1994).
743 84. PRINTS. http://www.bioinf.man.ac.uk/dbbrowser/PRINTS/
744 85. Hulo, N. *et al.* The PROSITE database. *Nucleic Acids Research* **34**, D227-D230
745 (2006).
746 86. PROSITE Database of protein domains, families and functional sites.
747 http://www.expasy.ch/prosite/.
748 87. Bru, C. *et al.* The ProDom database of protein domain families: more emphasis
749 on 3D. *Nucleic Acids Research* **33**, D212-D215 (2005).
750 88. ProDom. http://prodom.prabi.fr/.
751 89. Letunic, I., Doerks, T. & Bork, P. SMART 7: recent updates to the protein
752 domain annotation resource. *Nucleic Acids Research* **40**, D302-D305 (2012).
753 90. Simple Modular Architecture Research Tool. http://smart.embl-heidelber.de/.
754 91. Mi, H.Y. *et al.* The PANTHER database of protein families, subfamilies,
755 functions and pathways. *Nucleic Acids Research* **33**, D284-D288 (2005).
756 92. PANTHER Classification System. http://www.pantherdb.org/.
757 93. InterPro: protein sequence analysis & classification.
758 http://www.ebi.ac.uk/interpro/.
759 94. Ashburner, M. *et al.* Gene Ontology: tool for the unification of biology. *Nature*
760 *Genetics* **25**, 25-29 (2000).
761 95. The Gene Ontology Resource. http://geneontology.org/.
762 96. Ogata, H. *et al.* KEGG: Kyoto Encyclopedia of Genes and Genomes. *Nucleic*
763 *Acids Research* **27**, 29-34 (1999).
764 97. KEGG: Kyoto Encyclopedia of Genes and Genomes.
765 https://www.genome.jp/kegg/.
766 98. Li, L., Stoeckert, C.J. & Roos, D.S. OrthoMCL: Identification of ortholog groups
767 for eukaryotic genomes. *Genome Research* **13**, 2178-2189 (2003).
768 99. OrthoMCL. https://orthomcl.org/orthomcl/.
769 100. Edgar, R.C. MUSCLE: multiple sequence alignment with high accuracy and high
770 throughput. *Nucleic Acids Research* **32**, 1792-1797 (2004).
771 101. Stamatakis, A. RAxML-VI-HPC: Maximum likelihood-based phylogenetic
772 analyses with thousands of taxa and mixed models. *Bioinformatics* **22**, 2688-2690
773 (2006).

774 102. Stamatakis, A., Hoover, P. & Rougemont, J. A rapid bootstrap algorithm for the
775 RAxML web servers. *Systematic Biology* **57**, 758-771 (2008).
776 103. Yang, Z. PAML 4: Phylogenetic analysis by maximum likelihood. *Molecular
777 Biology and Evolution* **24**, 1586-1591 (2007).
778 104. Phylogenetic Analysis by Maximum Likelihood. Vol. 2017.
779 105. Hedges, S.B., Marin, J., Suleski, M., Paymer, M. & Kumar, S. Tree of life reveals
780 clock-like speciation and diversification. *Molecular Biology and Evolution* **32**,
781 835-845 (2015).
782 106. TimeTree. http://www.timetree.org.
783 107. De Bie, T., Cristianini, N., Demuth, J.P. & Hahn, M.W. CAFE: a computational
784 tool for the study of gene family evolution. *Bioinformatics* **22**, 1269-1271 (2006).
785 108. Computational Analysis of gene Family Evolution.
786 https://sourceforge.net/projects/cafehahnlab/.
787 109. Augustus web interface. http://bioinf.uni-greifswald.de/augustus/submission.php.
788 110. Kumar, S., Stecher, G. & Tamura, K. MEGA7: Molecular evolutionary genetics
789 analysis version 7.0 for bigger datasets. *Molecular Biology and Evolution* **33**,
790 1870-1874 (2016).
791 111. Liu, W. *et al.* IBS: an illustrator for the presentation and visualization of
792 biological sequences. *Bioinformatics* **31**, 3359-3361 (2015).
793 112. Vandesompele, J. *et al.* Accurate normalization of real-time quantitative RT-PCR
794 data by geometric averaging of multiple internal control genes. *Genome biology* **3**,
795 research0034 (2002).
796 113. Livak, K.J. & Schmittgen, T.D. Analysis of relative gene expression data using
797 real-time quantitative PCR and the 2(T)(-Delta Delta C) method. *Methods* **25**,
798 402-408 (2001).
799 114. Nielsen, H. Predicting Secretory Proteins with SignalP. in *Protein Function
800 Prediction: Methods and Protocols*, Vol. 1611 (ed. Kihara, D.) 59-73 (2017).
801 115. SignalP 4.1 Server. www.cbs.dtu.dk/services/SignalP-4.1/.
802 116. KNOTTIN database. http://www.dsimb.inserm.fr/KNOTTIN/.
803 117. Addgene. http://www.addgene.org/.
804 118. Liu, S., Ding, Z., Zhang, C., Yang, B. & Liu, Z. Gene knockdown by intro-
805 thoracic injection of double-stranded RNA in the brown planthopper, Nilaparvata
806 lugens. *Insect Biochemistry and Molecular Biology* **40**, 666-671 (2010).

807 119.Garcia, E., Rios, C. & Sotelo, J. Ventricular injection of nerve growth-factor
808 increase dopamine content in the striata of MPTP-treated mice. *Neurochemical*
809 *Research* **17**, 979-982 (1992).
810 120.Coddington, J.A., Agnarsson, I., Hamilton, C.A. & Bond, J.E. Spiders did not
811 repeatedly gain, but repeatedly lost, foraging webs. *Peerj* **7** (2019).

812 ## Figure legend

813 **Fig. 1. *P. pseudoannulata* and gene gain-and-loss analysis among species of**
814 **Arthropoda. (a)** A *P. pseudoannulata* catching prey. **(b)** The divergence time was
815 estimated by PAML mcmctree and is marked with a scale in million years. All
816 internal branches of the tree are 100% bootstrap supported. The numbers next to the
817 branch represent the numbers of expanded (green) and contracted (red) gene families
818 since the split from a most recent common ancestor.

819 **Fig. 2. Characterization of spridroin genes in *P. pseudoannulata*. (a)** Phylogeny
820 and gene structure characteristics of the *P. psedoannulata* spidroins. The phylogenetic
821 tree was constructed with the 130 N-terminal amino acid residues from each putative
822 gene product and transformed cladogram. Gene structures are drawn to scale. The
823 alternated grey and light grey blocks represent only the repeat regions without any
824 sequence preference. Only the N-terminal region and partial repeat region are
825 available for gene MaSp_16938. **(b)** The anatomy of the four types of silk glands in *P.*
826 *pseudoannulata*. Major ampullate gland (Ma), minor ampullate gland (Mi), aciniform
827 gland (Ac) and piriform gland (Pi) were dissected from a female spider. **(c)** The
828 relative expression of each spidroin gene type in female and male *via* qPCR.

829 **Fig. 3. Evolutionary analysis of neurotoxins from *P. pseudoannulata* and other**
830 **spiders.** Neurotoxins are categorized according to their target organism as
831 invertebrate only (red), vertebrate only (green) and both invertebrate and vertebrate
832 (blue). **(a)** Phylogeny of neurotoxins from *P. pseudoannulata* and other spiders.

833 Neurotoxins with known target organisms were used as a reference for target
834 organism prediction and are marked with red squares, green circles and blue
835 pentagons. Branches containing these neurotoxins were shaded accordingly. An
836 asterisk marks U1-lycotoxin-Pp1b. **(b)** Distribution of *P. pseudoannulata* neurotoxin
837 subtypes in terms of gene numbers. **(c)** Expression of different *P. pseudoannulata*
838 neurotoxin subtypes as the FPKM value in the venom gland transcriptome. **(d)** The
839 percentage of invertebrate-selective neurotoxins negatively correlated with spider
840 prosoma length. Horizontal bars represent the percentage of neurotoxins based on
841 their target organism selectivity. The black data points indicate prosoma length of the
842 predator spider. **(e)** Diversity of toxin composition in four spiders.
843

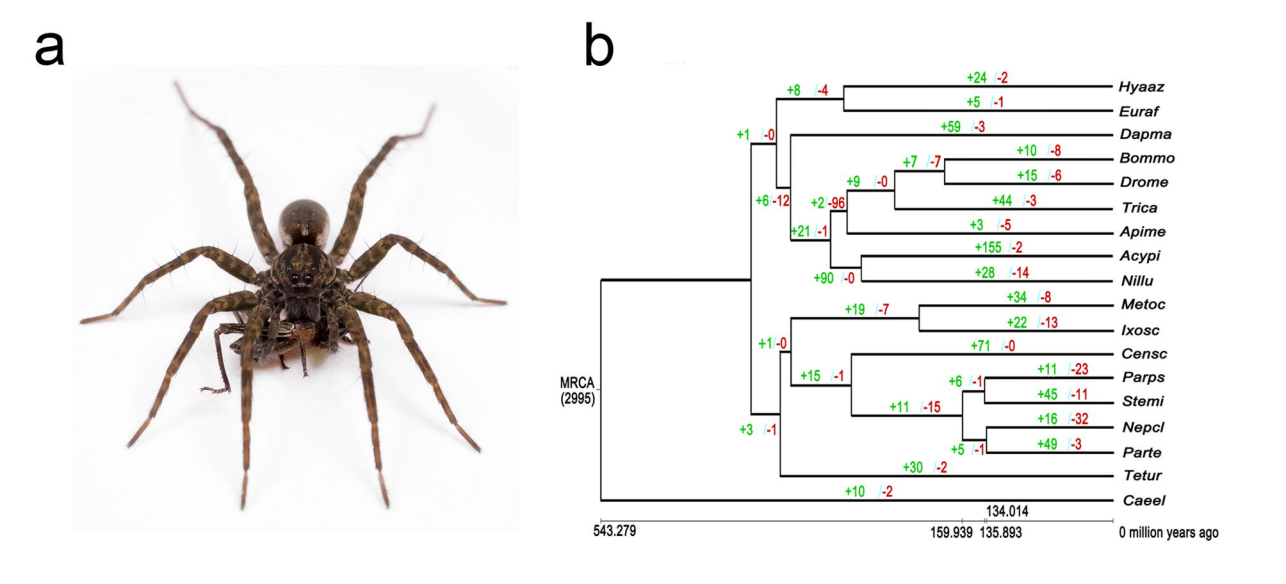
a
b
MRCA
(2995)
+8 -4
+24 -2
Hyaaz
+5 -1
Euraf
+1 -0
+59 -3
Dapma
+10 -8
Bommo
+7 -7
+15 -6
Drome
+9 -0
+6 -12
+2 -96
+44 -3
Trica
+3 -5
Apime
+21 -1
+155 -2
Acypi
+90 -0
+28 -14
Nillu
+34 -8
Metoc
+19 -7
+22 -13
Ixosc
+1 -0
+71 -0
Censc
+11 -23
+15 -1
+6 -1
Parps
+45 -11
Stemi
+11 -15
+16 -32
Nepcl
+3 -1
+49 -3
Parte
+5 -1
+30 -2
Tetur
+10 -2
Caeel
134.014
543.279
159.939 135.893
0 million years ago

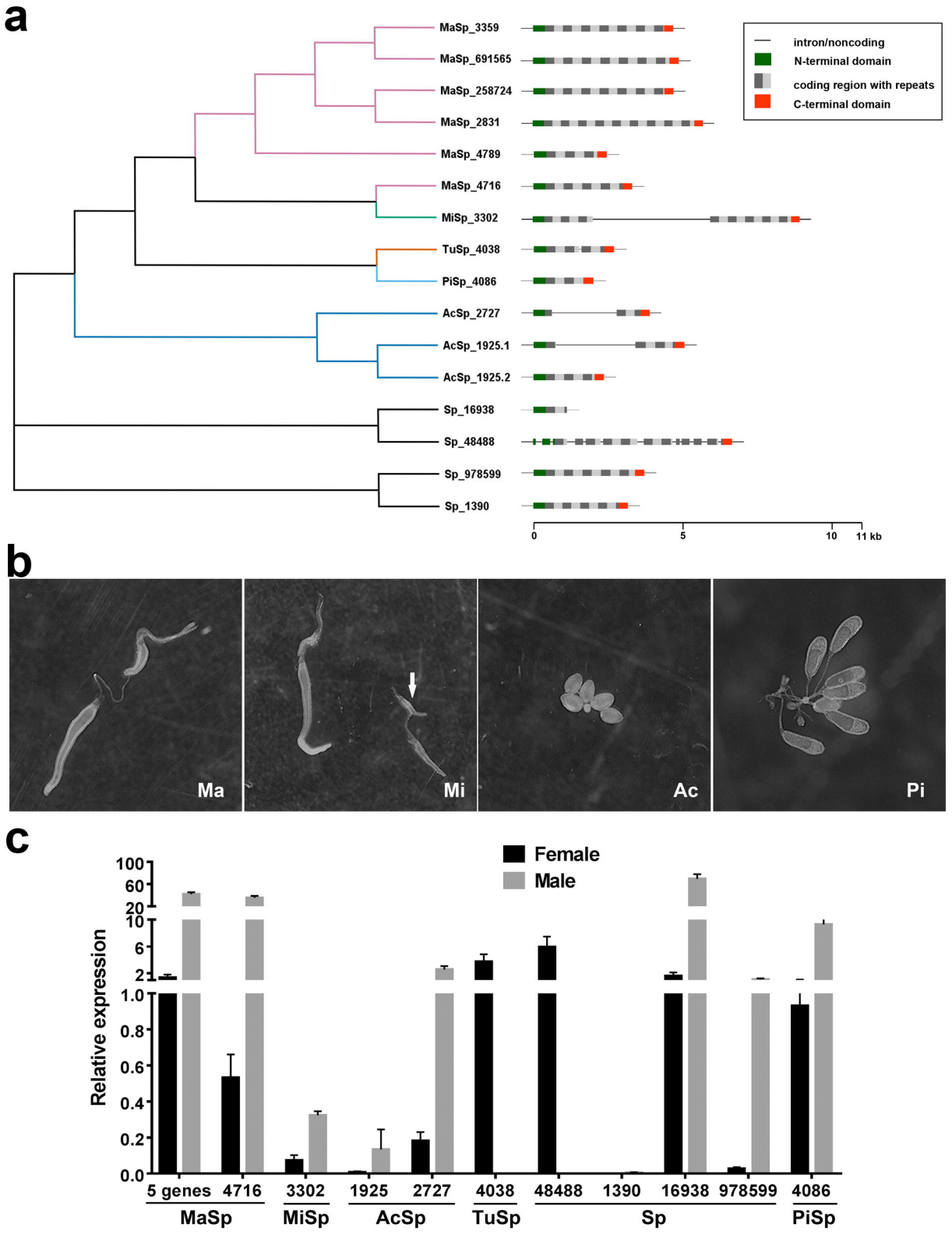
a
MaSp_3359
MaSp_691565
MaSp_258724
MaSp_2831
MaSp_4789
MaSp_4716
MiSp_3302
TuSp_4038
PiSp_4086
AcSp_2727
AcSp_1925.1
AcSp_1925.2
Sp_16938
Sp_48488
Sp_978599
Sp_1390
intron/noncoding
N-terminal domain
coding region with repeats
C-terminal domain
0
5
10
11 kb
b
Ma
Mi
Ac
Pi
c
Female
Male
Relative expression
100
60
20
10
6
2
1.0
0.8
0.6
0.4
0.2
0.0
5 genes
4716
3302
1925
2727
4038
48488
1390
16938
978599
4086
MaSp
MiSp
AcSp
TuSp
Sp
PiSp

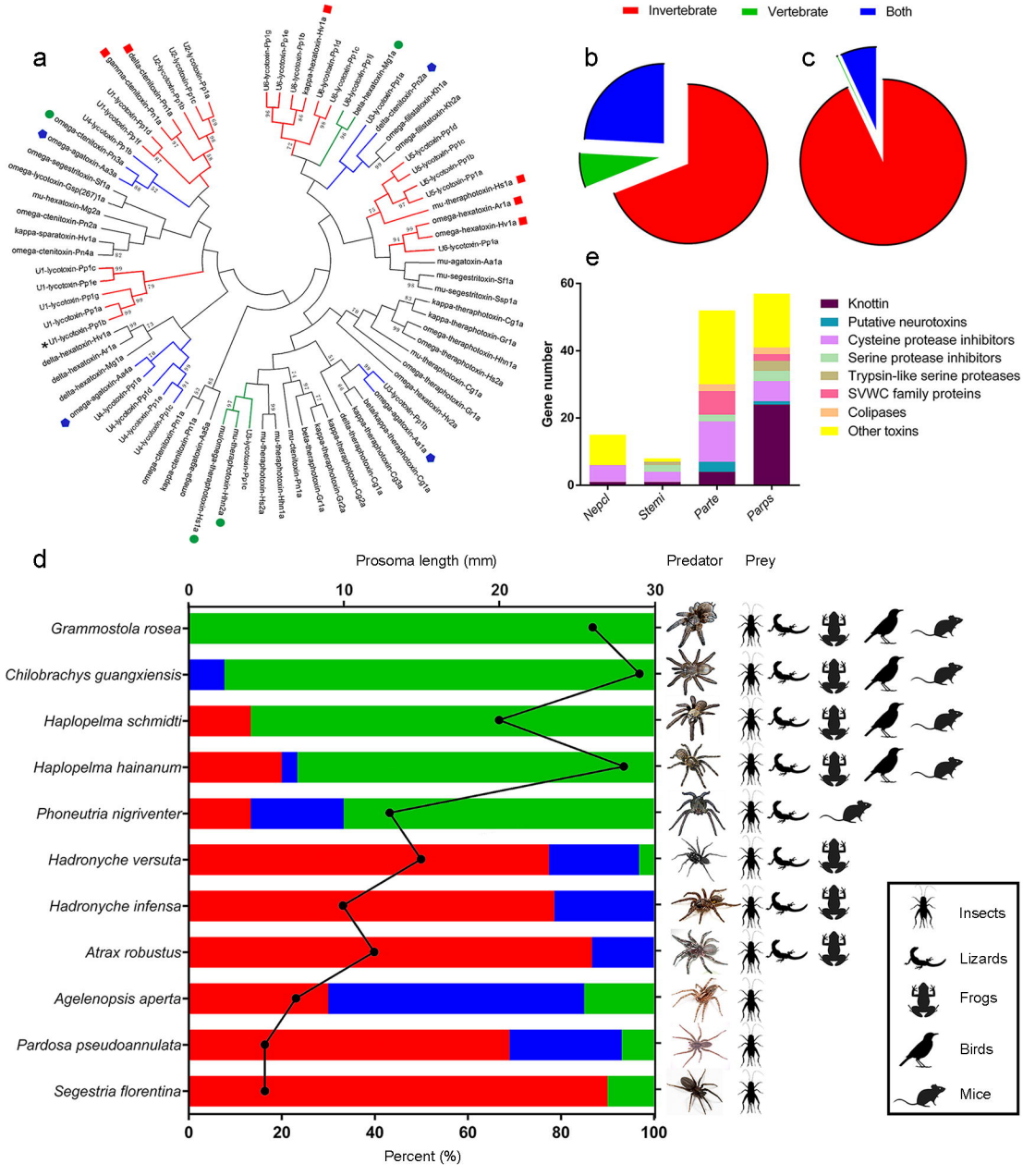
a
b
c
Invertebrate
Vertebrate
Both
e
Gene number
Knottin
Putative neurotoxins
Cysteine protease inhibitors
Serine protease inhibitors
Trypsin-like serine proteases
SVWC family proteins
Colipases
Other toxins
Nepcl
Sterni
Parte
Parps
d
Prosoma length (mm)
Predator
Prey
Grammostola rosea
Chilobrachys guangxiensis
Haplopelma schmidti
Haplopelma hainanum
Phoneutria nigriventer
Hadronyche versuta
Hadronyche infensa
Atrax robustus
Agelenopsis aperta
Pardosa pseudoannulata
Segestria florentina
Percent (%)
Insects
Lizards
Frogs
Birds
Mice